

Supporting Information

A novel biosensor for the monitoring of ovarian cancer tumor protein CA 125 in untreated human plasma samples using novel nano-ink: A new platform for efficient diagnosis of cancer

Arezoo Saadati ^{a,b}, Soodabeh Hassanpour ^c, Fanaz Bahavarnia ^{d,e,f}, Mohammad Hasanzadeh ^{a,*}

^a Pharmaceutical Analysis Research Center, Tabriz University of Medical Sciences, Tabriz, Iran.

^b Food and Drug Safety Research Center, Tabriz University of Medical Sciences, Tabriz, Iran.

^c Department of Analytical Chemistry, Faculty of Science, Palacky University Olomouc, 17. listopadu 12, 77146 Olomouc, Czech Republic.

^d Biotechnology Research Center, Tabriz University of Medical Sciences, Tabriz, Iran.

^e Nutrition Research Center, Tabriz University of Medical Sciences, Tabriz, Iran.

^f Liver and Gastrointestinal Diseases Research Center, Tabriz University of Medical Sciences, Tabriz, Iran.

Corresponding author.

M. Hasanzadeh (hasanzadehm@tbzmed.ac.ir)

Synthesis of DPA-GQDs

Functionalized GQDs are in the centre of attention since they play pivotal role in quantum dots characterization. Functionalization of GQD enhances functional potential, electronic, chemical and optical properties of quantum dots ¹. Two steps including pyrolysing acid citric and covalent reaction between GQD and the extra groups are required to synthesize functionalized GQDs. However, this procedure is time consuming. Moreover, it is unstable since consists some oxygen groups causing less functionalization degree.

To overcome the above problems, we used a one-step method for synthesizing DPA-GQD. In this study, thermal pyrolysis of the mixture citric acid and D-penicillamine was conducted in 200°C. Therefore, fluorescence intensity and stability of GQD increased as a result of DPA active groups. The optical and electrochemical properties of this probe relies on the ratio of DPA and citric acid (DPA/CA). In other words, more amount of citric acid results in big graphene sheets with perfect structure. However, less amount of citric acid results in less functionalization. Besides, the more amount of DPA lead to, the high degree of functionalization and the small size of graphene sheets. Therefore, GQDs may not be prepared in excessive mass ratio of DPA and citric acid. Different type of DPA-GQDs can be synthesized by different ratios of DPA and citric acid ².

Structure characterization

3.3. Fluorescence intensity and photo-stability

Fluorescence intensity and photo-stability of DPA-GQD was examined by fluorescence spectrometer. The UV absorption spectrum of DPA-GQD exhibits a strong peak at 363 nm. Beside, fluorescence spectrometer exhibits fluorescence excitation and emission for each ion in different concentration. According to Figure S1, an interesting point is that, DPA-GQD solution exhibits very high fluorescence intensity in comparison of pure GQD moreover, the

fluorescence intensities of DPA-GQD solution increases as a result of long lasting reaction time.

Also, DPA-GQDs was characterized by DLS, AFM, FTIR and. UV absorption spectra and peak fluorescence intensities of DPA/GQD were measured after successive dilution method and preparation transparent DPA-GQD solution. It has been revealed that the peak of absorption was appeared in 363 nm after 10 min incubation on the UV absorption and fluorescence intensities have been measured by spectrofluorimetric. The fluorescence intensities of DPA-GQD solution increases as a result of long lasting reaction time, in comparison of pure GQD.

DPA-GQD has two-dimensional sheet shape with a low degree of accumulation. The average particle size of DPA-GQD obtained by DLS was 1.11 nm (Figure S2 (see supporting information))).

AFM images and roughness analysis (Figure S3 (a,b) (see supporting information)) of synthesized GQD and DPA-GQD indicates that, GQDs has single monolayer thin structure. Because of size range of below 10 nm and 90% of GQDs particles represented dark brown. Moreover, the prepared DPA-GQD has thickness of 2-13 nm, which liaise to single-layer of functionalized GQDs also, it contains large amount of DPA-groups which are preponderantly located in the edges of graphene layers (See Table S1 (see supporting information)).

Fourier transform infrared spectroscopy (FT-IR) (Figure S4 (see supporting information)) Pattern of GQD and DPA-GQD reveals the functional groups of GQD and functionalized GQD.

There is distinct increase in the intensity of the N-H stretching signal and an appearance of SH₃ stretching signal from DPA-GQD. Furthermore, mass difference of functionalized groups reveals the presence of amino groups like -NH₂/-CH₃.

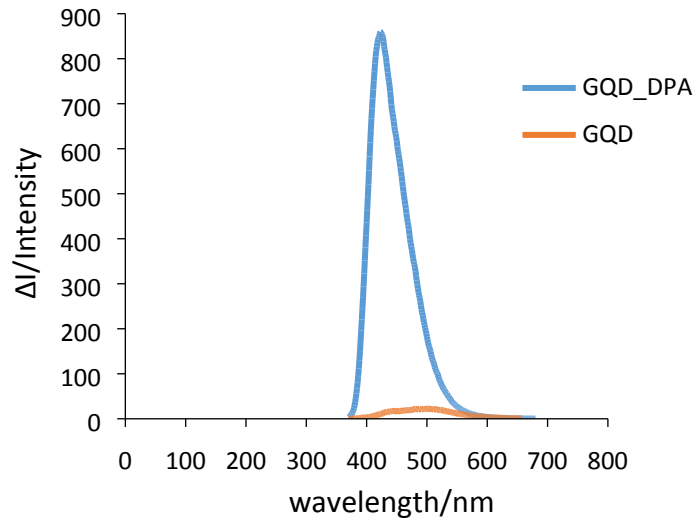


Fig. S1. Comparison of fluorescence intensities of GQD and DPA-GQD

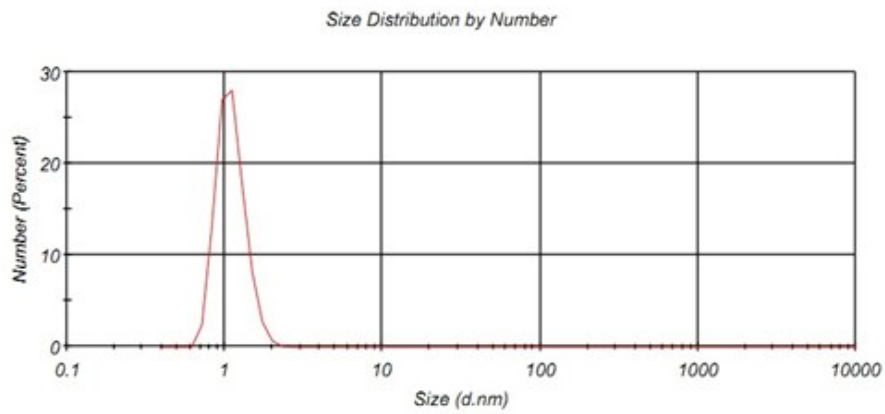


Fig. S2. DLS analysis of DPA-GQDs (100 ppm).

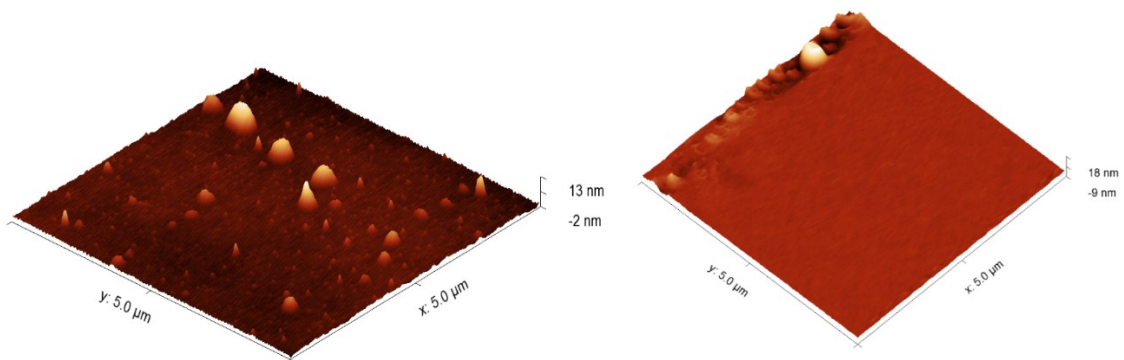


Fig. S3a,b. AFM images of GQD and DPA-GQD

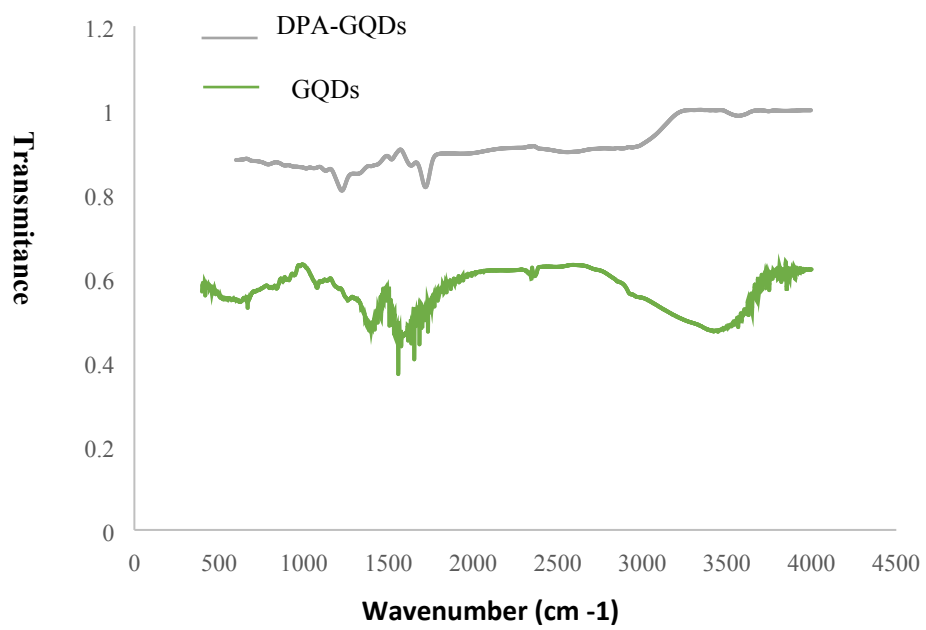


Fig. S4. FTIR of GQD and DPA-GQDs.

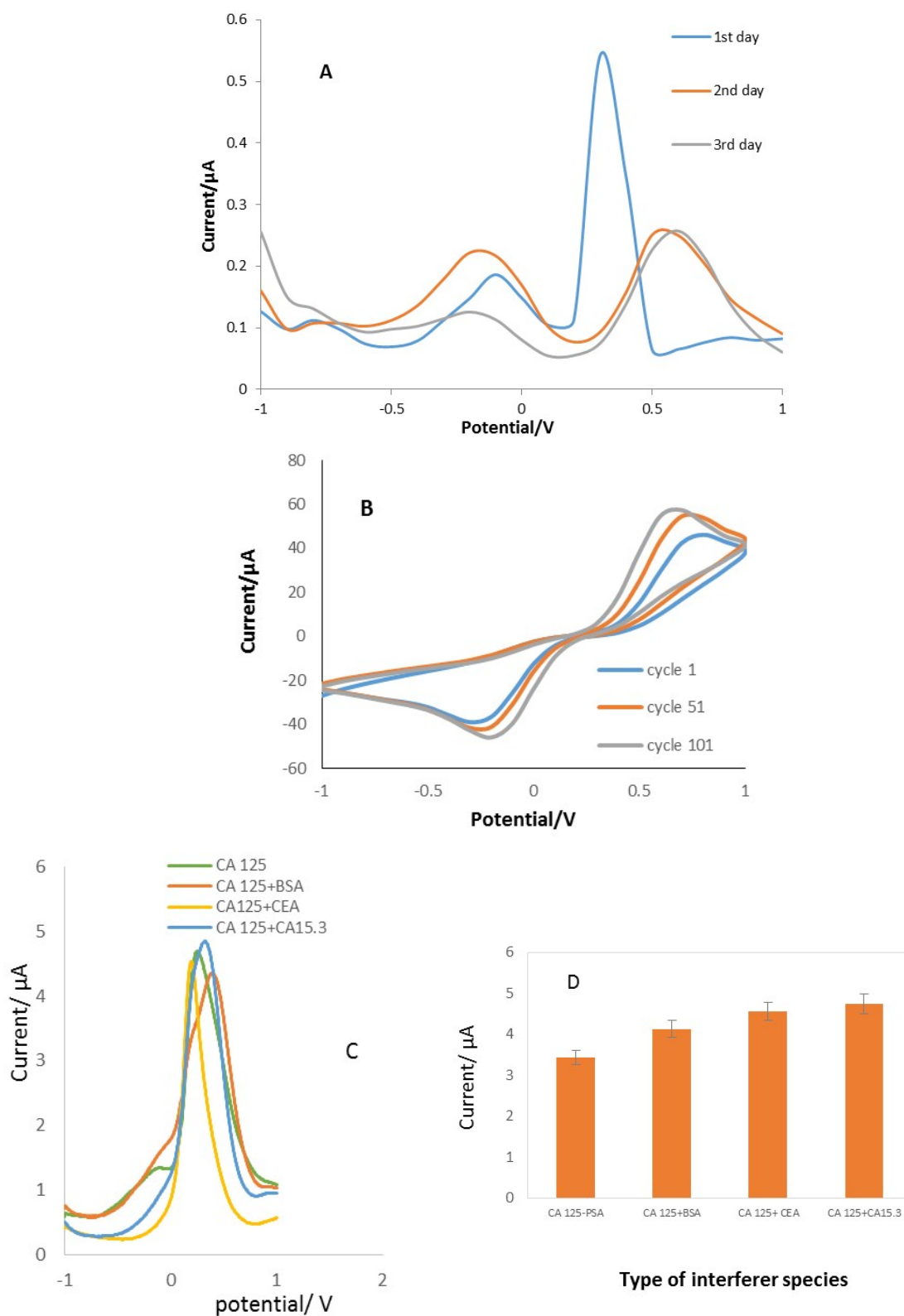


Fig. S5. **A)** DPVs of Ab/CysA-Au NPs/Ag-DPA-GQDs/GCE in different time of storage. $t_{\text{eq}}=2$ s, $E_{\text{begin}}=-1$ V, $E_{\text{end}}=1$ V, $E_{\text{step}}=0.1$ V, $E_{\text{pulse}}=0.005$ V, $t_{\text{pulse}}=0.2$ s, scan rate= 0.02 V/s. **B)** CVs of CysA-Au NPs/Ag-DPA-GQDs/GCE in various cycle number. Supporting electrode= $[\text{Fe}(\text{CN})_6]^{3-/4-}$ containing KCl. **C)** DPVs of the Ab/CysA-Au NPs/Ag-DPA-GQDs/GCE in the presence of some serum proteins (BSA, CA15.3, CA125 and PSA). **D)** Histogram of peak currents versus type of interfering species.

Table S1. Roughness analysis of AFM images.

R_a (nm)	Window dimensions (micron)	
3.37	1	GQD
1.20	5	GQD
1.39	10	GQD
0.352	1	DPA-GQD
0.482	5	DPA-GQD
11.3	10	DPA-GQD

References

1. S. Zhu, Y. Song, X. Zhao, J. Shao, J. Zhang and B. Yang, *Nano research*, **2015**, 8, 355-381.
2. W. Xuan, L. Ruiyi, F. Saiying, L. Zaijun, W. Guangli, G. Zhiguo and L. Junkang, *Sensors and Actuators B: Chemical*, **2017**, 243, 211-220.